International Journal of Computational and Theoretical Chemistry
2024, Vol. 12, No. 1, pp. 1-9
https://doi.org/10.11648/j.ijctc.20241201.11

Research Article

A DFT/TD-DFT Study of the Influence of Anchoring Group and Internal Acceptor of Benzocarbazole-based D-A´-π-A Dyes for DSSCs

Hanane Etabti*, Asmae Fitri, Adil Touimi Benjelloun, Mohammed Benzakour, Mohammed Mcharfi

Systems Engineering, Modeling and Analysis Laboratory, Faculty of Sciences Dhar El Mahraz, Sidi Mohamed Ben Abdellah University, Fez, Morocco

Abstract

Great attention is being shifted to Dye-sensitized solar cells because of their structural and electronic tunability, high performance, and low cost compared to conservative photovoltaic devices. In this work, the DFT/B3LYP/6-31G(d,p) and TD-DFT/mPW9PW91/6-31G(d,p) levels of theory are applied to the theoretical study of a new class of benzocarbazole-based D-A ´-π-A dyes for their potential use in DSSCs. The influence of the internal acceptor on the optoelectronic properties is studied for the dyes. The optoelectronic and photovoltaic properties as HOMO, LUMO, E_{gap} maximum absorption wavelength (λ_{max}), vertical excitation energies (E_{ex}), oscillator strength (*f*), light harvesting efficiency (LHE), open circuit voltage (V_{oc}), injection force (ΔG_{inject}), were evaluated and discussed in order to compare their performance as DSSC sensitizers. The theoretical results show that all dyes exhibit excellent optoelectronic properties, such as a lower E_{gap}(1.733 eV to 2.173 eV), a significant λ_{max}(631.48 nm to 754.40 nm), a sufficient value of V_{oc} (0.461 V to 0.880 V) and high LHE (0.853 eV to 0.968 eV). In particular M4 with 2,5-dihydropyrrolo [3,4-c]pyrrole-1,4-dithione as auxiliary acceptor has the potential to be used as a sensitizer for DSSCs, due to its red-shifted absorption spectrum (λ_{max}= 754.40 nm), and small energy gap (E_{gap}=1.733 eV). Indeed, this study may help chemists to synthesize efficient dyes for DSSC.

Keywords

Benzocarabzole, DFT/TD-DFT, Auxiliary Acceptor, Photovoltaic Properties, Dye-sensitized Solar Cells

1. Introduction

Currently, solar energy is recognized as the most plentiful among renewable sources, offering significant potential in mitigating challenges stemming from fossil fuels and other environmentally troublesome energy sources [1, 2]. As the third generation solar cells, dye-sensitized solar cells (DSSCs) developed by O'Regan and Gratzel in 1991, have attracted

*Corresponding author: etabti.hanane@gmail.com (Hanane Etabti)

Received: 3 December 2023; **Accepted:** 15 January 2024; **Published:** 29 April 2024

considerable attention in both academia and commercial industry due to their safe fabrication mechanism and ideal PCE [3]. One of the key design parameters of DSSCs is the dye sensitizer, which plays a critical role in photo-electric conversion processes with the functions of light harvesting, electron injection, electrons collection and dye regeneration [3-5]. So far, sensitizers are divided into two sub-groups: metal-based dyes [6, 7] and metal-free organic dyes [8, 9]. Previously, metal-based dyes (Ru and Zn) were widely used due to their high power conversion efficiency (PCE) [6, 10]. Nevertheless, these metal-based dyes are having an adverse effect on the environment and complex purification processes lead to their limited applications in DSSCs [11]. To address this issue, scientists and researchers are directing their attention toward metal-free organic dyes because of their minimal toxicity, high molar extinction coefficient, ease of accessibility, lightweight properties, and cost-effectiveness. [12]. The reported PCE for these metal-free organic dyes reached up to 14% having a donor-π-acceptor (D-π-A) structure anchored on the surface TiO_2 [11]. Among these metal-free sensitizers, carbazole and its derivatives, with advantages of strong emission and adsorption properties, good hole transport capacities and reasonable band gaps [13], have been proved to be promising candidates for DSSCs efficiency. In this context, several studies have shown that PCEs of carbazole sensitizing dyes can reach 9.20% [14, 15]. Conversely, the efficiency of Dye-Sensitized Solar Cells (DSSCs) is significantly influenced by the molecular structure of the dye. In recent developments, the creation of novel organic dyes adopting the D-A-π-A configuration involves incorporating an internal acceptor into conventional D-π-A dyes [16-18]. The Studies on D-A-π-A dyes show that the additional internal electron-withdrawing acceptor can be considered as an electron trap having unique characteristics [19]. Insertion of an electron-withdrawing internal group in the D-π-A arrangement not only tunes the absorption energies and energy levels, but also improves the photostability of the sensitizers [11]. Moreover, in DSSCs, the sensitizers directly interact with a mesoporous oxide layer made of nanometre-sized particles (usually TiO_2-anatase) through anchoring groups. Therefore, the search for different anchoring groups with the excellent binding ability to the semiconductor is essential to replace conventional carboxylic acid-based anchoring groups such as cyanoacrylic acid because this last is prone to photodegradation during device operation as they dissociate from semiconductor's surface [2, 20]. Based on the theoretical researches of slimi et al. [21] and G. Deogratias et al. [22], results showed that 2-(1,1-dicyanomethylene) rhodanine unit is a very promising anchoring group for improving photovoltaic properties of dye sensitizers.

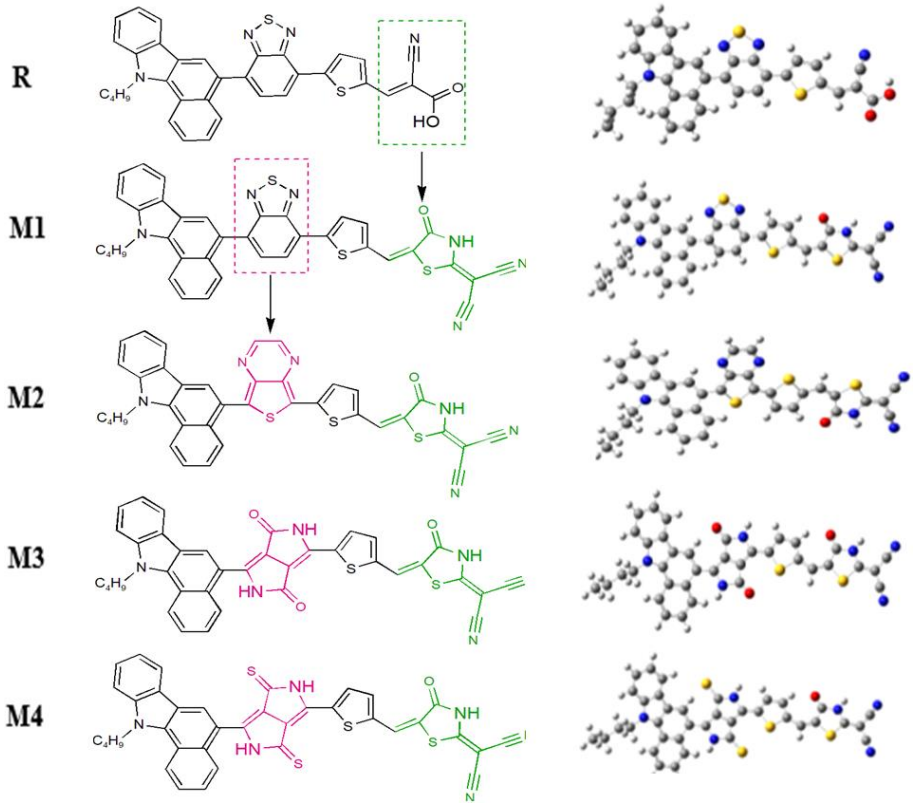

Figure 1. *(a) Molecular structure of studied dyes; and (b) their optimized geometry with DFT at the B3LYP/6-31G(d,p) level.*

In this work, with the goal to evaluate the effect of internal acceptors on the performance of benzocarbazole dyes, a serious of D-A'-π-A dyes are designed on the basis of LY-8 (R) dye [23], where D: benzocarbazole, A': benzothiadiazole (M1), 2-methylbenzotriazole (M2), 2,5-dihydropyrrolo [3,4-c] pyrrole-1,4-dione (M3) and 2,5-dihydropyrrolo [3,4-c] pyrrole-1,4-dithione (M4), π-bridge: thiophene, A: 2-(1,1-dicyanomethylene) rhodanine acid (Figure 1a). Theoretical insights into the inherent characteristics of the formulated dyes are provided through density functional theory (DFT) and time-dependent DFT (TD-DFT) methods. This encompasses analyses of molecular geometry, electronic structure, frontier molecular orbitals, absorption spectrum, light harvesting efficiency (LHE), and properties related to photo-induced electron transfer. The objective of this study is to elucidate the impact of internal acceptor types on the photoelectric performance of the dyes. The derived conclusions aim to offer valuable insights for the design and screening of innovative high-performance benzocarbazole dyes for Dye-Sensitized Solar Cells (DSSCs).

2. Computational Details

In this study, all computational calculations were conducted using the Gaussian 09 package [24]. Ground state geometry optimization of the dyes was performed through Density Functional Theory (DFT) calculations, employing the hybrid functional B3LYP [25] and the 6-31G (d,p) basis set [26], in the gas phase. Additionally, frequency calculations were executed to verify that the optimized structure represented the minimum energy configuration. For the computation of absorption spectra, Time-Dependent Density Functional Theory (TD-DFT) calculations were carried out with the mPW9PW91 [27] functional and a 6-31G(d,p) basis set, utilizing the optimized ground state geometries for the first excited singlet state. Solvation effects, including chloromethane (CH_3Cl), were incorporated, employing the Integral Equation Formalism Polarizable Continuum Model (IEF-PCM) [28]. This model is widely used in various studies to assess the optical properties of dyes [29, 30].

3. Results and Discussion

3.1. Optimized Ground-state Geometries

The optimized geometries of the studied dyes R, M1–M4 at a B3LYP/6-31G(d,p) level in their ground states are shown in Figure 1b. The values of the selected structural parameters (di and ϕi), mentioned in Scheme 1, were extracted and listed in Table 1. As shown in Scheme 1, ϕ_1 and d_1 are the dihedral angle and bond length between the donor (D) and internal acceptor (A′) respectively. ϕ_2 and d_2 are the dihedral angle and bond length between internal acceptor (A′) and π-spacers while ϕ_3 and d_3 are corresponding to the dihedral angle and bond length of π-spacer and anchoring acceptor (A).

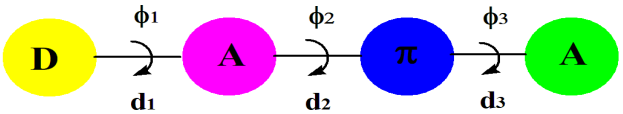

Scheme 1. *Model structure of D-A′-π-A dyes.*

Table 1. *Selected bond angles (in °) and bond lengths (in Å) of all the dyes calculated at B3LYP/6-31G(d,p) level of theory.*

Dye	ϕ_1	ϕ_2	ϕ_3	d_1	d_2	d_3
R	-50.25	1.61	0.01	1.481	1.456	1.426
M1	50.28	-1.76	0.03	1.481	1.455	1.429
M2	41.08	-0.52	-0.23	1.464	1.432	1.425
M3	-20.83	-2.20	0.48	1.449	1.430	1.429
M4	-31.06	-4.89	0.25	1.448	1.432	1.431

From Table 1, it can be observed that the dihedral angle (ϕ_1) for all the dyes vary between -50 °and 50 °. This non-planarity of the structure is important as it may reduce dye aggregation. Moreover, M2, M3 and M4 have smaller absolute value ϕ_1 (about 20 °– 40 °) than that of R and M1. It means that variation of the internal acceptor groups affects noticeably the process of charge transfer process from the donor (D) to the internal acceptor (A′). However, planarity is maintained between the

internal acceptor group and the π-bridge (ϕ_2), and between the π-bridge and the anchoring acceptor (ϕ_3). This planarity may facilitate intramolecular charge transfer from the π-bridge to the anchoring group. On the other hand, the inter-cyclic link lengths (d_1, d_2, d_3) are all about 1.4 Å. This value lies midway between the distances associated with a singular link and a double link. The reduction in length is attributed to the impact of conjugation within the examined systems. The coplanar arrangement, coupled with the intramolecular charge transfer facilitated by the conjugation effect in these systems, is anticipated to enhance the likelihood of π-stacking and, consequently, facilitate charge transport.

3.2. Electronic Properties and Frontier Molecular Orbitals (FMOs)

In order to evaluate the efficiency of electron injection and regeneration of the sensitizers, the HOMOs, LUMOs and energy gaps of the investigated dyes were calculated and shown in Figure 2. Obviously, all molecules have higher LUMO than the conduction band (CB) of TiO_2 (−4.0 eV) [31], and lower HOMO than the redox potential of I^-/I_3^- (−4.8 eV) [32], which demonstrates that the excited dyes can be reduced by redox couple, and excited electrons can effectively inject to the CB of TiO_2. Therefore, all invested molecules are effective dyes. The energy gap (E_{gap}) was calculated as the difference between the energy levels HOMO and LUMO and is listed in Table 2. From this table, the energy gaps (E_{gap}) of all designed dyes decrease in the order: R (2.207 eV) > M1 (2.137 eV) > M2 (2.077 eV) > M3 (1.913 eV) > M4 (1.733 eV). It shows that the modification of the cyanoacrylic acid by 2-(1,1- dicyanomethylene) rhodanine acid unit in M1 has positive effet in the decrease of E_{gap} relative to R. Further, when changing the internal acceptor group the band gap is reduced greatly. The most interesting finding is the much lower E_{gap} value for M4 compared to other studied dyes; this is due to the strong electron-withdrowing ability of 2,5-dihydropyrrolo [3,4-c] pyrrole-1,4-dithione and lead to the electrons being more easily excited and thus favorable for getting bathochromic shift of the absorption band, which may make contributions to higher power conversion efficiency.

Table 2. *Energy values of HOMO, LUMO and E_{gap} of all dyes.*

Dye	E_{HOMO}(eV)	E_{LUMO}(eV)	E_{gap}(eV)
R	-5.327	-3.120	2.207 (2.13)[a]
M1	-5.326	-3.189	2.137
M2	-5.230	-3.152	2.077
M3	-5.186	-3.273	1.913
M4	-5.272	-3.539	1.733
TiO_2	-	-4.000	-

[a] Experimental values in parentheses are from ref [23]

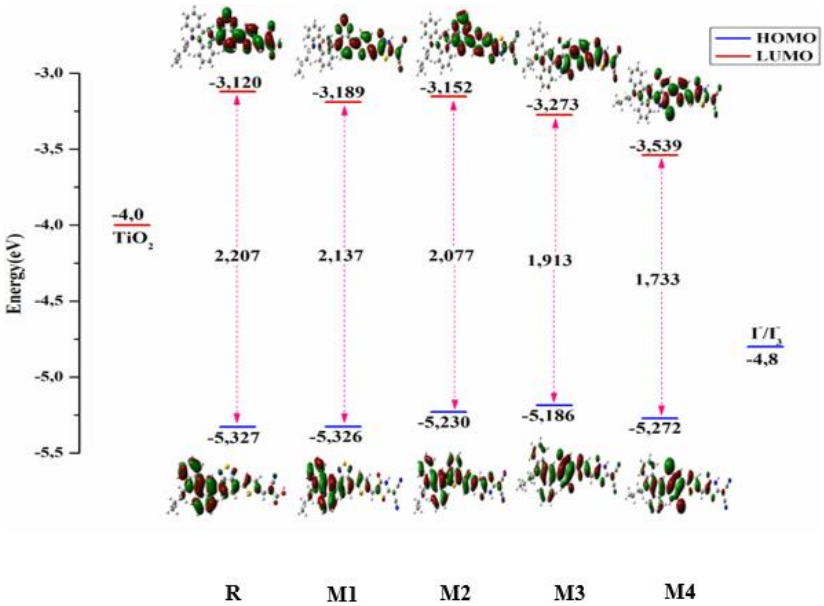

Figure 2. *Sketch of B3LYP/6-31G (d,p) calculated energies of the HOMO, LUMO level of studied dyes.*

To gain an insight into the intramolecular charge transfer (ICT), the frontier molecular orbitals (FMOs) of HOMO and LUMO are depicted in Figure 2. From this figure we observe that in the electron distributions of HOMOs are localized on donor, internal acceptor and spacer unit, while the LUMOs are essentially localized on internal acceptor, spacer and anchoring acceptor unit. Examination of the HOMO and LUMO of these dyes indicates that HOMO–LUMO excitation moves the electron distribution from the donor unit to the acceptor.

3.3. Photovoltaic Properties

Overall efficiency of photo-elution conversion in DSSCs is determined by the integral for J_{SC} (short-circuit photocurrent density), V_{oc} (open circuit photovoltage), FF (fill factor) and P_{inc} (incident photon to current efficiency) from equation [33]:

$$\eta = \frac{J_{sc} V_{oc} FF}{P_{inc}} \quad (1)$$

Therefore, η can be enhanced by increasing J_{SC} and V_{oc}.

Theoretically, the maximum open circuit photovoltage (V_{oc}) of the DSSC is determined by the difference between the LUMO of the donor (E_{LUMO} of the dye) and the LUMO of the acceptor $E_{CB} = -4.0$ eV [31] of the conduction band of semiconductor TiO_2) according to the following relationship [34]:

$$V_{oc} = E_{LUMO} - E_{CB} \quad (2)$$

On the other hand, J_{SC} is related to the efficiency of electron injection ϕ_{inj}, the charge collective efficiency ($\eta_{collect}$) and the light harvesting efficiency at a given wavelength (LHE) via the following expression [35]:

$$J_{sc} = \int_{\lambda} LHE\ (\lambda)\ \phi_{inj}\ \eta_{collect}\ d\lambda \quad (3)$$

For the same DSSCs with only different dyes, it is reasonable to assume that $\eta_{collect}$ is constant [36]. However, to know theoretically the relation between the J_{sc} and η, we have studied the LHE and ϕ_{inj} from Eq. (3), to obtain a high J_{sc}, the efficient dyes used in DSSCs must have a large LHE that can be expressed as follows [37]:

$$LHE = 1\text{-}10^{-f} \quad (4)$$

while *f* represents the oscillator strength of dye molecules at a specific wavelength.

For a larger light-harvesting efficiency (LHE), the oscillator strength obtained must be greater. In addition, a large ϕ_{inj} based on Eq. (3) could give a J_{sc}. The ϕ_{inj} is linked to the driving force of the injection ΔG_{inject} by [36, 38, 39]:

$$\Delta G_{inject} = E^{dye^*} - E_{CB} = E^{dye} - E_{00} - E_{CB} \quad (5)$$

where E^{dye*} and E^{dye} are the oxidation energy of the excited dye and the oxidation potential energy of the dye in ground state, respectively. While E_{00} is electronic vertical transition energy corresponding to λ_{max}.5)

Table 3. *Estimated electrochemical parameters for all dyes.*

Dye	E^{dye}	E^{dye*}	ΔG_{inject}	LHE	V_{oc}
R	5.327	3.355	-0.645	0.737	0.880
M1	5.326	3.363	-0.637	0.853	0.811
M2	5.230	3.388	-0.612	0.925	0.848
M3	5.186	3.415	-0.585	0.968	0.727
M4	5.272	3.628	-0.371	0.888	0.461

The parameters mentioned above (E^{dye}, E^{dye*}, ΔG_{inject}, LHE and V_{oc}) of all the dyes were calculated and presented in Table 3. From this table, the E^{dye*} energy values increase in the order R < M1 < M2 < M3 < M4, revealing that the R dye is the most readily oxidized molecule among the studied dyes, while M4 is the least. For ΔG_{inject}, a larger absolute value of ΔG_{inject} will be conducive to the electron injection and then improve the J_{SC}. As shown in Table 3, all values are negative, this shows that charge injection are thermodynamically favorable for all designed dyes. The ΔG_{inject} energy values increase in the order: R < M1 < M2 < M3 < M4. In comparison to R, the ΔG_{inject} value increased (less negative) when replacing the cyanoacrilic acid by 2-(1,1-dicyanomethylene) rhodanine acid, in dye M1 (-0.637 eV). Further when changing the internal acceptor group, the driving force for injection ΔG_{inject} is heighten greatly to -0.612, -0.585, -0.371 eV, in M2, M3, M4, respectively; therefore, the order of the driving force of the dyes is R > M1 > M2 > M3 > M4. To get an overview of the photocurrent performance of these dyes, the light-harvesting efficiency (LHE) should be as large as possible to maximize the photocurrent response. From Table 3, we can see that M2 (0.925) and M3 (0.968) display the largest LHE, which makes these designed dyes exhibit stronger light absorption capacity. On the other hand, the values of open-circuit photovoltage (V_{oc}) of the studied dyes range from 0.461 eV to 0.880 eV,

these values are sufficient for a possible efficient electron injection of electrons into the LUMO of the TiO_2 semiconductor.

3.4. Optical Properties

Table 4. *TD-DFT data of R dye calculated using different functionals.*

Functional	λ_{max}a/(nm)	εa /(M-1.cm-1)
B3LYP	455, 676	30466, 21228
BHandLYP	386, 498	21963, 41746
CAM-B3LYP	381, 484	19263, 44112
PBE0	502, 921	22378, 15295
mPW1PW91	437, 628	31248, 23900
Experimental*	405, 489	33269, 20545

[a] Maximum absorption wavelength λ_{max} and molar extinction coefficient at λ_{max} of dyes
* Experimental values in CH_3Cl [23]

Table 5. *Computed absorption maxima (λ_{max}), excitation energies (E_{ex}), oscillator strengths (f) and the contribution of the most probable transition of the studied dyes in chloromethane solvent using TD/ mPW1PW91/6-31G(d,p) level of theory.*

Dye	λ_{max}(nm)	E_{ex}(eV)	f	Main composition
R	628.58	1.972	0.582	H → L (0.69)
	437.66	2.833	0.735	H-2 → L (0.69)
M1	631.48	1.963	0.835	H → L (0.69)
	471.73	2.628	0.904	H-1 → L (0.63)
M2	673.11	1.842	1.128	H → L (0.70)
	482.58	2.569	0.661	H-1 → L (0.52)
M3	699.75	1.772	1.498	H → L (0.70)
	410.08	3.023	0.489	H-3 → L (0.66)
M4	754.40	1.644	0.953	H → L (0.70)
	503.92	2.460	0.136	H → L+1 (0.53)

H= HOMO; L= LUMO; H-1=HOMO-1; H-2=HOMO-2; H-3=HOMO-3; L+1=LUMO+1

The determination of the optical properties of these dyes is carried out by TD-DFT method. For the consideration of the reliability of theoretical method, five different functionals were used, including B3LYP, BHandLYP, CAM-B3LYP, PBE0 and mPW1PW91. Table 4 shows the resulted maximal absorptions for R at different functionals in comparison with the experimental absorption. The λ_{max} obtained at mPW1PW91 functional is closer to the experimental spectrum; therefore, mPW1PW91 functional was the most reliable to investigate the absorption spectra. So, the absorption spectra for all of dyes were calculated at mPW1PW91/6-31G(d,p) method. The calculated data of absorption wavelengths (λ_{max}), electronic vertical transition energies (E_{ex}) and oscillator strengths (*f*) of all dyes in solvent

(CH_3Cl) were carried out and listed in Table 5 and the corresponding simulated absorption spectra illustrated in Figure 3.

We can see that all the dyes absorb in the visible and assign to the ICT transitions. Compared with dye R, the substitution of the cyanoacrylic acid group (R: 602 nm) by 2-(1,1-dicyanomethylene) rhodanine moiety (M1: 593 nm) weakly affects the value of λ_{max}. Further when changing the internal acceptor group the absorption spectra is more redshifted. In the case of M2, the incorporation of 2-methylbenzotriazole unit displays a remarkable 42 nm red-shifting absorption than benzothiadiazole (M1). 2-methylbenzotriazole is expected to be a stronger electron-deficient unit than benzothiadiazole. Also, M3 showed a more red-shifted absorption of 68 nm than M1, which might enhance the light harvesting of the sensitizers. For, dye M4 displays a 123 nm red-shifted absorption band when compared to dye M1, due to the fact that the 2,5-dihydropyrrolo [3,4-c]pyrrole-1,4-dithione unit is a much stronger p-electron deficient unit also by their great electronic affinity.

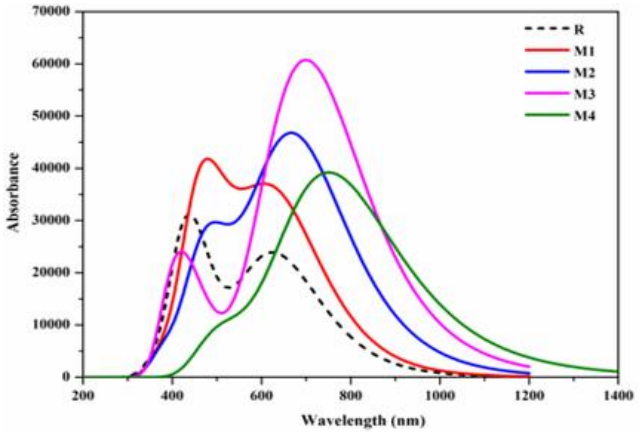

Figure 3. *Calculated UV-Visible absorption spectra in chloromethane of all dyes by mPW1PW91/6-31G(d,p).*

4. Conclusions

The Density functional theory (DFT) and time-dependent DFT (TD-DFT) methods have been used to investigate the performance of some benzocarbazole-based dyes as sensitizers in the dye-sensitized solar cells (DSSCs). The geometry structures, energy levels, absorption information, ICT property and electrons recombination process have been analyzed. Results showed that variation of functionalized internal acceptor (A') had a significant effect on the optoelectronic and chemical properties. The designed molecules M1-M4 showed smaller energy gaps (from 2.137 to 1.733 eV), improved intramolecular charge transfer between electron donor and acceptor and enlarged absorption range in the visible region (from 631.48 to 754.40 nm) compared to R (2.207 eV/ 628.58nm).

For new designed benzocarbazole-based dyes, M4 containing 2,5-dihydropyrrolo [3,4-c]pyrrole-1,4-dithione will display better energetic, electronic and optical parameters compared with original molecules R and designed molecules M1-M3 for application in DSSC. The investigation provides guidance for experimental synthesis and developed new high-performance materials in the fields of DSSCs and photocatalysis.

Conflicts of Interest

The authors declare no conflicts of interest.

References

[1] G. Li, L. Sheng, T. Li, J. Hu, P. Li, K. Wang, Engineering flexible dye-sensitized solar cells for portable electronics, *Sol. Energy* 177 (2019), 80–98.

[2] G. Deogratias, N. Seriani, T. Pogrebnaya, A. Pogrebnoi, Tuning optoelectronic properties of triphenylamine based dyes through variation of pi-conjugated units and anchoring groups: A DFT/TD-DFT investigation, *J. Mol. Graph. Model.* 94 (2020), 107480.

[3] D. Zhao, R. M. Saputra, P. Song, Y. Yang, F. Ma, Y. Li, Enhanced photoelectric and photocatalysis performances of quinacridone derivatives by forming D-π-A-A structure, *Sol. Energy* 201 (2020), 872–883.

[4] S. Ahmad, E. Guillén, L. Kavan, M. Grätzel, M. K. Nazeeruddin, Metal free sensitizer and catalyst for dye sensitized solar cells, *Energy Environ. Sci.* 6 (2013), 3439–3466.

[5] Z. Xu, S. Gao, X. Lu, Y. Li, Y. Li, S. Wei, Theoretical analysis of the absorption spectrum, electronic structure, excitation, and intramolecular electron transfer of D–A′–π–A porphyrin dyes for dye-sensitized solar cells, *Phys. Chem. Chem. Phys.* 22 (2020), 14846–14856.

[6] S. Mathew, A. Yella, P. Gao, R. Humphry-Baker, B. F. E. Curchod, N. Ashari-Astani, I. Tavernelli, U. Rothlisberger, M. K. Nazeeruddin, M. Grätzel, Dye-sensitized solar cells with 13% efficiency achieved through the molecular engineering of porphyrin sensitizers, *Nat. Chem.* 6 (2014), 242–247.

[7] W. Zeng, Y. Cao, Y. Bai, Y. Wang, Y. Shi, M. Zhang, F. Wang, C. Pan, P. Wang, Efficient dye-sensitized solar cells with an organic photosensitizer featuring orderly conjugated ethylenedioxythiophene and dithienosilole blocks, *Chem. Mater.* 22 (2010), 1915–1925.

[8] C. Sun, y. Li, j. Han, B. Cao, H. Yin, Y. Shi, Enhanced photoelectrical properties of alizarin-based natural dye via structure modulation, *Sol. Energy* 185 (2019), 315–323.

[9] L. J. He, Y. Sun, W. Li, J. Wang, M. X. Song, H. X. Zhang, Highly-efficient sensitizer with zinc porphyrin as building block: Insights from DFT calculations, *Sol. Energy* 173 (2018), 283–290.

[10] C. Y. Chen, M. Wang, J. –Y. Li, N. Pootrakulchote, L. Alibabaei, C. –H. Ngoc-le, J. –D. Decoppet, J. –H. Tsai, C. Grätzel, C. –G. Wu, S. M. Zakeeruddin and M. Grätzel, Highly efficient light-harvesting ruthenium sensitizer for thin-film dye-sensitized solar cells, *ACS Nano* 3 (2009), 3103–3109.

[11] A. Tripathi, A. Ganjoo, P. Chetti, Influence of internal acceptor and thiophene based π-spacer in DA-π-A system on photophysical and charge transport properties for efficient DSSCs: A DFT insight, *Sol. Energy* 209 (2020), 194–205.

[12] G. Pepe, J. M. Cole, P. G. Waddell, J. R. D. Griffiths, Molecular engineering of fluorescein dyes as complementary absorbers in dye co-sensitized solar cells, *Mol. Syst. Des. Eng.* 1 (2016), 402–415.

[13] Y. H. Cui, Y. Tong, L. Han, J. Gao, J. K. Feng, Design and photoelectric properties of DA-π-A carbazole dyes with different π-spacers and acceptors for use in solar cells: a DFT and TD-DFT investigation, *J. Mol. Model.* 25 (2019), 249.

[14] J. Liu, X. Yang, A. Islam, Y. Numata, S. Zhang, N. T. Salim, H. Chen, L. Han, Efficient metal-free sensitizers bearing circle chain embracing π-spacers for dye-sensitized solar cells, *J. Mater. Chem.* A 1 (2013), 10889–10897.

[15] H. Etabti, A. Fitri, A. Touimi Benjelloun, M. Hachi, M. Benzakour, M. Mcharfi, Benzocarbazole-based D–Di–π–A dyes for DSSCs: DFT/TD-DFT study of influence of auxiliary donors on the performance of free dye and dye–TiO_2 interface, *Res. Chem. Intermed.* 47 (2021), 4257–4280.

[16] Y. Wu, W. H. Zhu, S. M. Zakeeruddin, M. Grätzel, Insight into D–A− π–A structured sensitizers: a promising route to highly efficient and stable dye-sensitized solar cells, *ACS Appl. Mater. Interfaces* 7 (2015), 9307–9318.

[17] X. Wang, J. Yang, H. Yu, F. Li, L. Fan, W. Sun, Y. Liu, Z. Y. Koh, J. –H. Pan, W. –L. Yim, L. Yan, Q. Wang, A benzothiazole–cyclopentadithiophene bridged D–A–π–A sensitizer with enhanced light absorption for high efficiency dye-sensitized solar cells, *Chem. Commun.* 50 (2014), 3965–3968.

[18] Y. Gao, X. Li, Y. Hu, Y. Fan, J. Yuan, N. Robertson, J. Hua, S. R. Marder, Effect of an auxiliary acceptor on D–A–π–A sensitizers for highly efficient and stable dye-sensitized solar cells, *J. Mater. Chem.* A 4 (2016), 12865–12877.

[19] C. C. Chiu, Y. C. Sheng, W. J. Lin, R. Juwita, C. J. Tan and H. H. Gavin Tsai, *ACS Omega* 3 (2018), 433–445.

[20] T. Higashino, Y. Fujimori, K. Sugiura, Y. Tsuji, S. Ito, H. Imahori, Tropolone as a high‐performance robust anchoring group for dye‐sensitized solar cells, *Chemie* 127 (2015), 9180–9184.

[21] H. Etabti, A. Fitri, A. Touimi Benjelloun, M. Benzakour, M. Mcharfi, Designing and Theoretical Study of Dibenzocarbazole Derivatives Based Hole Transport Materials: Application for Perovskite Solar Cells, *Journal of Fluorescence* 33 (2023), 1201-1216.

[22] H. Etabti, A. Fitri, A. Touimi Benjelloun, M. Benzakour, M. Mcharfi, Effects of the terminal donor unit on the photovoltaic parameters of benzocarbazole-based dyes for DSSCs: DFT/TD-DFT investigations, E3S Web of Conferences 336 (2022), 00031.

[23] L. Han, J. Liu, Y. Liu, Y. Cui, Novel DA-π-A type benzocarbazole sensitizers for dye sensitized solar cells, *J. Mol. Struct.* 1180 (2019), 651–658.

[24] M. J. Frisch, G. W. Trucks, H. B. Schlegel, G. E. Scuseria, M. A. Robb, J. R. Cheeseman, G. Scalmani, V. Barone, B. Mennucci, G. A. Petersson, H. Nakatsuji, M. Caricato, X. Li, H. P. Hratchian, A. F. Izmaylov, J. Bloino, G. Zheng, J. L. Sonnenberg, M. Hada, M. Ehara, K. Toyota, R. Fukuda, J. Hasegawa, M. Ishida, T. Nakajima, Y. Honda, O. Kitao, H. Nakai, T. Vreven, J. A. Jr. Montgomery, J. E. Peralta, F. Ogliaro, M. Bearpark, J. J. Heyd, E. Brothers, K. N. Kudin, V. N. Staroverov, R. Kobayashi, J. Normand, K. Raghavachari, A. Rendell, J. C. Burant, S. S. Iyengar, J. Tomasi, M. Cossi, N. Rega, J. M. Millam, M. Klene, J. E. Knox, J. B. Cross, V. Bakken, C. Adamo, J. Jaramillo, R. Gomperts, R. E. Stratmann, O. Yazyev, A. J. Austin, R. Cammi, C. Pomelli, J. W. Ochterski, R. L. Martin, K. Morokuma, V. G. Zakrzewski, G. A. Voth, P. Salvador, J. J. Dannenberg, S. Dapprich, A. D. Daniels, O. Farkas, J. B. Foresman, J. V. Ortiz, J. Cioslowski, D. J. Fox, Gaussian 09. Gaussian, Inc., Wallingford CT 32 (2009), 5648–5652.

[25] C. Lee, W. Yang, R. G. Parr, Development of the Colle-Salvetti correlation-energy formula into a functional of the electron density, *PHYSICAL REVIEW B* 37 (1988).

[26] A. D. Becke, *J. Chern. Phys.* 98 (1993).

[27] C. Adamo, V. Barone, Exchange functionals with improved long-range behavior and adiabatic connection methods without adjustable parameters: The mPW and mPW1PW models, *J. Chem. Phys.* 108 (1998), 664‐675.

[28] J. Tomasi, B. Mennucci, E. Cancès, The IEF version of the PCM solvation method: an overview of a new method addressed to study molecular solutes at the QM ab initio level, *J. Mol. Struct.* 464 (1999), 211–226.

[29] H. Etabti, A. Fitri, A. Touimi Benjelloun, M. Benzakour, M. Mcharfi, Efficient tuning of benzocarbazole based small donor molecules with D-π-A-π-D configuration for high-efficiency solar cells via π-bridge manipulation: a DFT/ TD-DFT study, *comput. theor. chem.* 1208 (2022), 113580.

[30] H. Etabti, A. Fitri, A. Touimi Benjelloun, M. Benzakour, M. Mcharfi, Designing and theoretical study of benzocarbazole-based D-π-D type small molecules donor for organic solar cells, Journal of Molecular Graphics and Modelling 121 (2023), 108455.

[31] M. Grätzel, World Scientific, (2011).

[32] S. Kim, J. K. Lee, S. O. Kang, J. Ko, J. –H. Yum, S. Fantacci, F. D. Angelis, D. D. Censo, M. K. Nazeeruddin, M. Grätzel, Molecular engineering of organic sensitizers for solar cell applications, *J. Am. Chem. Soc.* 128 (2006), 16701–16707.

[33] D. Chattopadhyay, S. Lastella, S. Kim, F. Papadimitrakopoulos, Length separation of zwitterion-functionalized single wall carbon nanotubes by GPC, *J. Am. Chem. Soc.* 124 (2002), 728–729.

[34] W. Sang-aroon, S. Saekow, V. Amornkitbamrung, Density functional theory study on the electronic structure of Monascus dyes as photosensitizer for dye-sensitized solar cells, *Journal Photochem. Photobiol. A Chem.* 236 (2012), 35–40.

[35] S. Chen, L. Yang, Z. Li, How to design more efficient organic dyes for dye-sensitized solar cells? Adding more sp2-hybridized nitrogen in the triphenylamine donor, *J. Power Sources* 223 (2013), 86–93.

[36] J. Zhang, H. –B. Li, S. –L. Sun, Y. Geng, Y. Wu, Z. -M. Su, Density functional theory characterization and design of high-performance diarylamine-fluorene dyes with different π spacers for dye-sensitized solar cells, *J. Mater. Chem.* 22 (2012), 568–576.

[37] Z. Zhang, L. Zou, A. Ren, Y. Liu, J. Feng, C. Sun, Theoretical studies on the electronic structures and optical properties of star-shaped triazatruxene/heterofluorene co-polymers, *Dye. Pigment.* 96 (2013), 349–363.

[38] W. Fan, D. Tan, W. Deng, Acene‐modified triphenylamine dyes for dye‐sensitized solar cells: a computational study, *ChemPhysChem* 13 (2012), 2051–2060.

[39] J. Xu, L. Zhu, D. Fang, B. Chen, L. Liu, L. Wang, W. Xu, Substituent effect on the π linkers in triphenylamine dyes for sensitized solar cells: a DFT/TDDFT study, *ChemPhysChem* 13 (2012), 3320–3329.